An Experimental Approach to Systematically Probe Charge Inversion in Nanofluidic Channels

Kuang-Hua Chou[+], Christopher McCallum[+], Dirk Gillespie[^], Sumita Pennathur[+][*]

[+] University of California, Santa Barbara, CA, 93106 USA

[^] Rush University Medical Center, Chicago, IL, 60612 USA

sumita@ucsb.edu

Theoretical Model

All equations are solved in COMSOL 5.2 (COMSOL, Inc., Stockholm, Se), fully coupled, over a wide range of values for each parameter as listed in Table 1. The spatiotemporal-varying ζ-potential is specified by three parameters: $\zeta_1 = -43$ mV (as found experimentally for Tris buffer), ζ_2 (the ζ-potential of the charge-inverting inflow electrolyte), and t_{ads} (the adsorption time of charge-inverting species).

Table S1: Parameters used in simulations.

Parameter	minimum	maximum	step size
ζ_2 (mV)	0.0	13	0.05
t_{ads} (s)	5.0	90	2

We perform simulations to match the experimental results and extract these parameters. The species concentration time evolution is determined by the Nernst-Planck equation:

$$\frac{\partial c_i}{\partial t} + \nabla \cdot \left(-D_i \nabla c_i - \frac{z_i D_i F}{RT} c_i E \right) + u \cdot \nabla c_i = 0 \tag{1}$$

where c_i is the concentration of species i, D_i is the diffusivity, z_i is the charge, F is the Faraday constant, R is the gas constant, T is temperature, E is the electric field, and u is the velocity. We use a one-dimensional geometry and solve for the electric field from Gauss's Law,

$$\nabla \cdot J = 0, \ J = \sigma E, \ E = -\nabla V \tag{2}$$

where J is the current density, σ is the conductivity (given from experimental values and varying in space with the concentration front), and V is the voltage. The fluid velocity is composed of electroosmotic flow (EOF) (assumed to be plug flow) and pressure-driven flow (PDF) components, $u = u_{EOF} + u_{PDF}$, with

$$u_{\text{EOF}} = -\frac{\varepsilon}{\eta} \zeta(x,t) E(x,t)$$

$$u_{\text{PDF}} = \frac{\partial p}{\partial x} \frac{h^2}{12\eta}$$
(3)

where ε is the permittivity, η is the viscosity (taken to be that of water), $\zeta(x,t)$ and $E(x,t)$ are the spatiotemporally-varying ζ-potential and electric field, and p is the pressure. We determine the pressure from the continuity equation:

$$\frac{\partial}{\partial x}\left(u_{\text{EOF}} + u_{\text{PDF}}\right) = 0$$
(4)

To specify the ζ-potential, we hypothesize that there are two important parameters that affect the current monitoring curve: 1) ζ_2, the steady-state ζ-potential that the charge inverting ion produces, and 2) t_{ads}, the time it takes for those ions to adsorb to the wall and change the ζ-potential. These parameters depend both on the concentration of charge-inverting ion in the channel and the speed of the concentration front. To understand how these two parameters can change the current monitoring curve, we show in Figure 3 numerical simulations of current monitoring with changing parameters ζ_2 and t_{ads}. We assume that the ζ-potential changes as a smooth function,

$$f(x,x_0 a) = \left(1 + \exp\left(-\frac{x - x_0}{a}\right)\right)^{-1}$$
(5)

where x_0 is the sigmoid's midpoint and a is its width. We can then write the ζ-potential as an explicit function:

$$\zeta(x,t,\zeta_1,\zeta_2,t_{\text{ads}}) = f(x,t \cdot u_{\text{EOF}}, t_{\text{ads}} \cdot u_{\text{EOF}}) \cdot \zeta_1 + \left(1 - f(x,t \cdot u_{\text{EOF}}, t_{\text{ads}} \cdot u_{\text{EOF}})\right) \cdot \zeta_2$$
(6)

where ζ will transition from ζ_1 to ζ_2 over an adsorption length $L_{\text{ads}} = t_{\text{ads}} \cdot u_{\text{EOF}}$ and propagate at the same speed as the concentration front, u_{EOF}. We solved the coupled set of equations for a wide range of ζ_2 and t_{ads} (given in Table S1) in COMSOL 5.2 (COMSOL, Inc., Stockholm, Se) for a one-dimensional channel geometry to simulate the current versus time in a nanochannel. The large resulting set of current versus time data is then compared (using a least-squares) to the experimental traces to extract both ζ_2 and t_{ads}.

Supplementary Data

Figure S1 shows an example current monitoring experiment in which 24.7 mM Tris buffer (100%) displaces 22.23 mM Tris buffer (90%) for a voltage of 30 V in a 100 nm channel. This characteristic experiment highlights the expected linear current versus time curve for a simple buffered solution. Figure S2 shows the range of ζ-potential of the charge inverting species, ζ_2, as well as the adsorption time, t_{ads}, for each concentration of Ru(bpy)$_3$Cl$_2$. Notably, the 0.1 mM case

shows a much larger t_{ads} relative to the higher concentrations, and ζ_2 increases for increasing concentration. This is in good agreement with our hypothesis, that more dilute systems will show delayed adsorption, as well as lower charge inversion. Table S2 shows all conductivity of solutions we used. Furthermore, Figure S3 shows the three results for the Ru(bpy)$_3$Cl$_2$ current monitoring experiments and best fit simulation matches for 0.1, 2.5, and 5 mM Ru(bpy)$_3$Cl$_2$. Both parameters, ζ_2 and t_{ads} are given for each experiment.

To accurately measure ζ-potential, we assume that the electroosmotic flow of the channel follows the Helmholtz-Smoluchowski equation for velocity,

$$u_{\text{EOF}} = -\frac{\varepsilon}{\eta}\zeta E. \tag{7}$$

To find u_{EOF} we simply measure the time it takes for the current to plateau (i.e., the time the fluid takes to traverse the length of the channel) and divide the length of the channel by this time to get the experimental area-average velocity (u_{EOF}). In the case of Figure S1, this time was 27.4 seconds and yielded an average ζ-potential (ζ_1) of –43±4.17 mV ($n > 10$). Note that the Helmholtz-Smoluchowski equation does make the assumption of thin electric double layers, but for the experiments performed in this study, the double layers never extend beyond 3 nm of the 100 nm channel (3% of the channel), so we assume them to be negligible for the purposes of this work.[1]
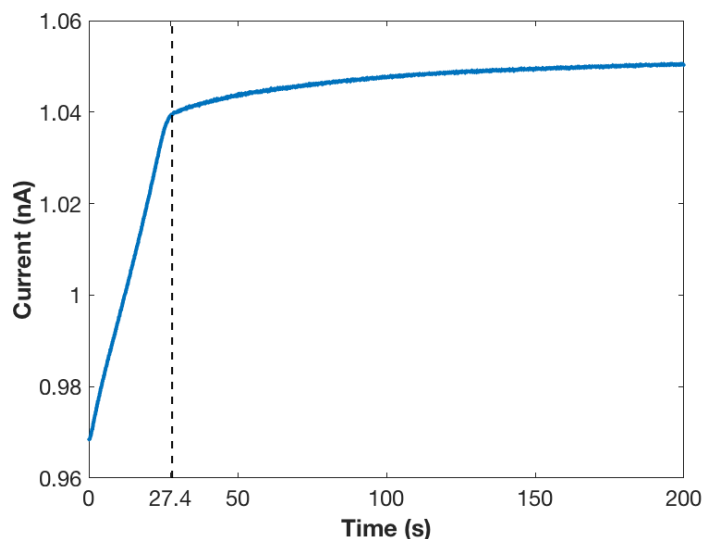

Figure S1: Typical current-monitoring (CM) experiment. When the channel was filled 22.23 mM (90%) Tris buffer, the positive well was replaced with 24.70 mM (100%) Tris buffer and the voltage, 30 V, applied simultaneously. The dashed vertical line indicates the time when the lower concentration solution has arrived at the positive well.
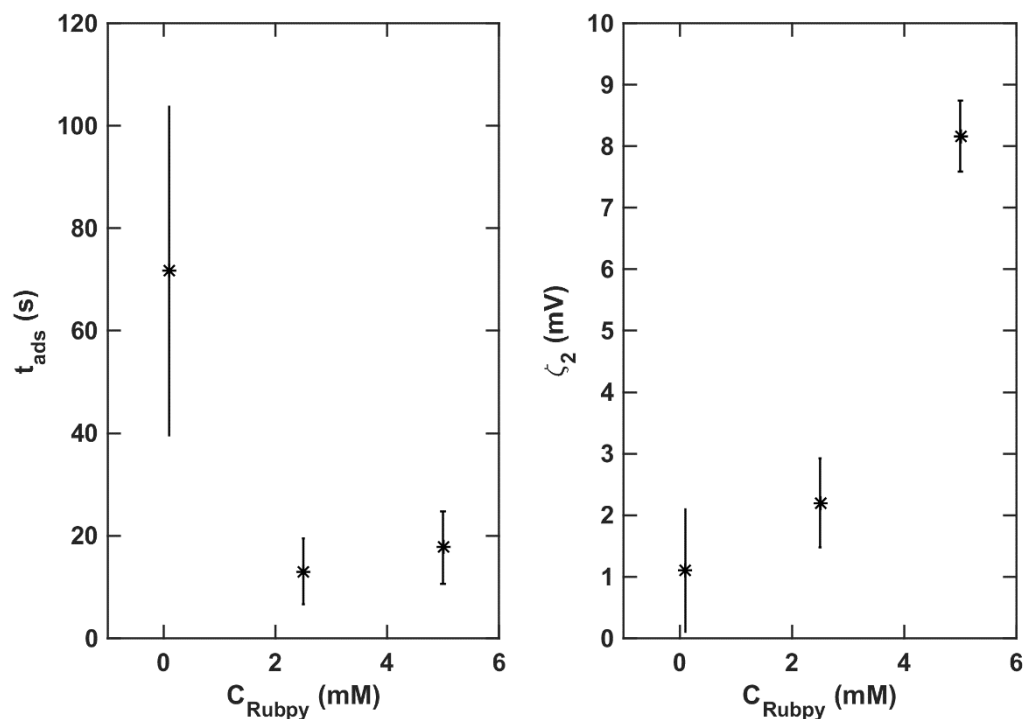
Figure S2: Distribution of t_{ads} and ζ_2 for different Ru(bpy)$_3$Cl$_2$ concentrations.   Each symbol is the mean of the fitted parameters for three experiments (the rows of Fig. S3), and the error bars are the SD of the fitted parameters.   We assume $\zeta_1 = -43$ mV.   A comprehensive error estimation of ζ_2 and t_{ads} should include propagation of the experimental error in ζ_1, but because we only use three experiments, the variance in the experimental data is relatively high and therefore here we only show the simplest error estimates.

**Table S2** All conductivity of solutions

Solutions	Conductivity
24.70 mM Tris (100%)	3.063 mS/cm
22.23 mM Tris (90%)	2.845 mS/cm
10 mM LaCl$_3$ + 10 mM Tris	4.068 mS/cm
20 mM LaCl$_3$ + 10 mM Tris	7.299 mS/cm
0.1 mM Ru(bpy)$_3$Cl$_2$ + 10 mM Tris	1.341 mS/cm
2.5 mM Ru(bpy)$_3$Cl$_2$ + 10 mM Tris	1.765 mS/cm
5.0 mM Ru(bpy)$_3$Cl$_2$ + 10 mM Tris	2.220 mS/cm
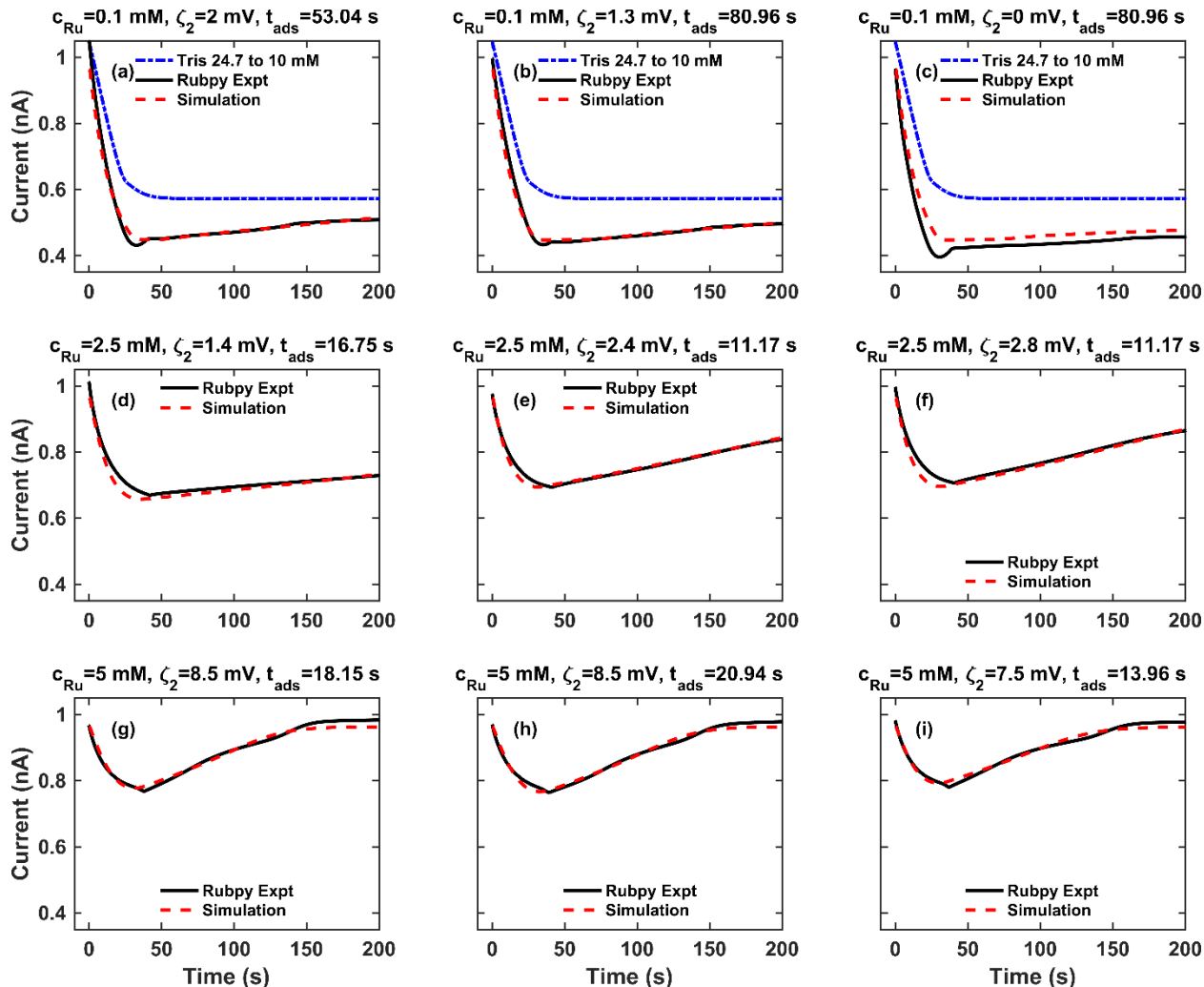
Figure S3: All Ru(bpy)$_3$Cl$_2$ experiments and corresponding simulation matches. (a)-(c) represents three different experiments with a Ru(bpy)$_3$Cl$_2$ concentration of 0.1 mM, and corresponding simulation best fits. Blue line represents a current monitoring curve with just Tris buffer with no Ru(bpy)$_3$Cl$_2$. (d)-(f) represents three different experiments with a Ru(bpy)$_3$Cl$_2$ concentration of 2.5 mM, and corresponding simulation best fits. (g)-(i) represents three different experiments with a Ru(bpy)$_3$Cl$_2$ concentration of 5 mM, and corresponding simulation best fits. After calculating results for many parameters, we minimized the L_2 norm of the difference between experimental and simulation data, and report percent RMSD as $100 L_2 (\text{simulation} - \text{experiment})/L_2 (\text{experiment})$. Specifically, this RMSD for each panel is (a) 1.41%, (b) 1.27%, (c) 11.35%, (d) 2.76%, (e) 0.92%, (f) 1.67%, (g) 3.47%, (h) 2.60%, and (i) 2.67%.

Density Function Theory (DFT)

Figure S4 shows that the ζ-potential can be changed with different concentrations of trivalent ion La^{3+}, becoming positive to induce a reversal of fluid flow.
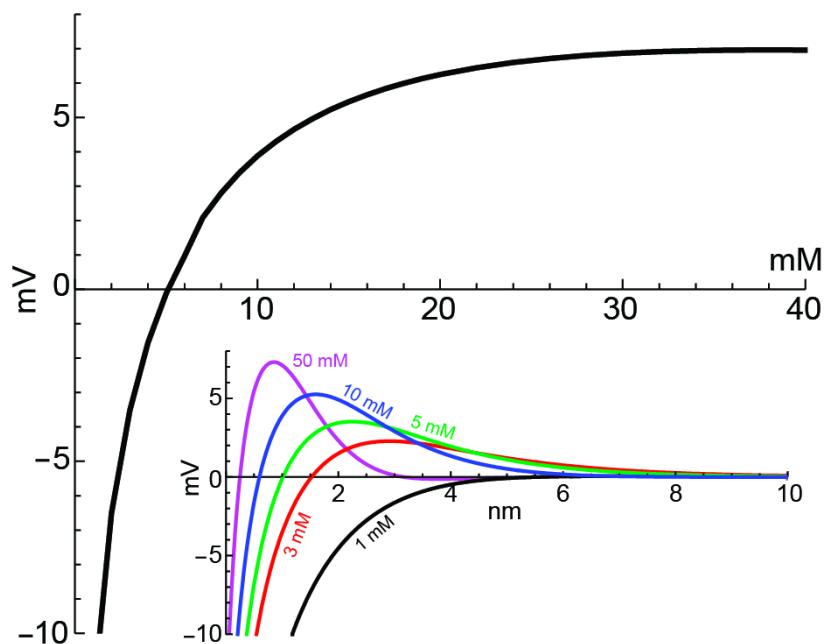
Figure S4. The inset shows the electrostatic potential as a function of distance from a wall with uniform surface charge -0.05 C/m^2 for a mixture of La^{3+} (diameter 0.15 nm)[2] and 10 mM Tris (diameter 0.7 nm).[3] The anion is Cl^-. $[La^{3+}]$ is 1 mM (black line), 3 mM (red), 5 mM (green), 10 mM (blue), and 50 mM (magenta). The main figure shows ζ-potential as a function of $[La^{3+}]$, specifically the electrostatic potential at 1 nm distance from the wall. As there is currently no theory for where the slip plane is located, we use 1 nm to illustrate how the sign of the ζ-potential can change. The ions are modeled as previously described.[4]

Images of the Experimental Device
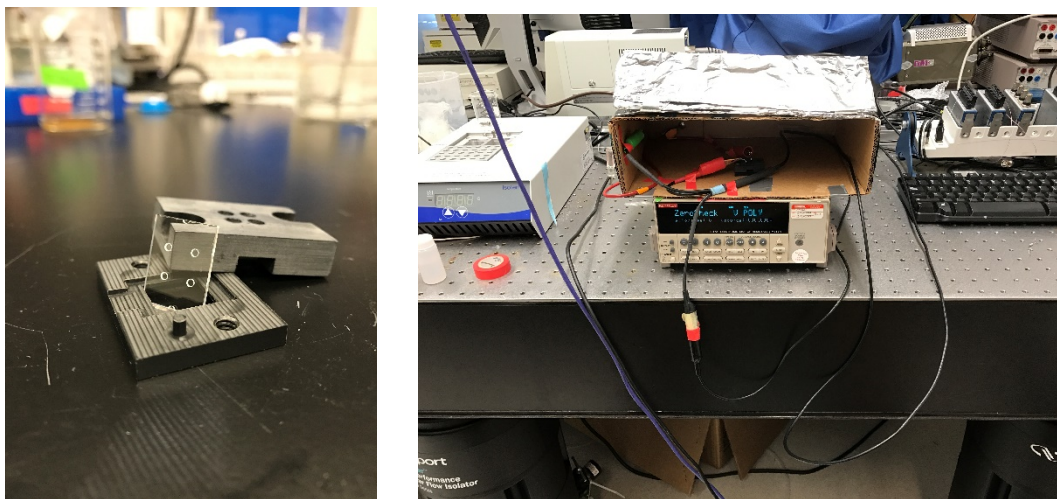
Figure S5. Images of our experimental device and setup. (Left) picture of nanochannel device (two channels per chip) resting against the acrylic machined chip holder. There are O-rings that help seal the channel into the chip holder. (Right) Image of experimental setup. We measure current with a Keithley 6517 electrometer and place the chip and chip holder in a Faraday cage with platinum electrode connections.

REFERENCES

1. Gaš, B., Štědrý, M., Kenndler, E. *Journal of Chromatography A* **1995,** 709, 63-68.
2. Shannon, R. D.; Prewitt, C. T. *Acta Crystallographica Section B Structural Crystallography and Crystal Chemistry* **1969,** 25, 925-946.
3. Tinker, A.; Lindsay, A. R., Williams, A. J. *J Gen Physiol* **1992,** 100, 495-517.
4. Roth, R.; Gillespie, D. *J Phys Condens Matter* **2016,** 28, 244006.